Vânia Brito, Tamerlan Saidov, Teresa Diaz Gonçalves, Leo Pel (accepted June 2014) NMR identification of sodium sulfate phases crystallizing on Ançã limestone under different environmental conditions. Journal of Building Physics, DOI: 10.1177/1744259114543981.

Delamination of Ançã limestone due to sodium sulfate under different environmental conditions as studied by NMR

Vânia Brito
Materials Department, National Laboratory for Civil Engineering (LNEC), Av. do Brasil 101 – Lisbon, Portugal
Email: vbrito@lnec.pt

Tamerlan A. Saidov
Department of Applied Physics, Eindhoven University of Technology, Eindhoven, The Netherlands
Email: t.saidov@tue.nl

Teresa Diaz Gonçalves*
Materials Department, National Laboratory for Civil Engineering (LNEC), Av. do Brasil 101 – Lisbon, Portugal
Email: teresag@lnec.pt
* corresponding author

Leo Pel
Department of Applied Physics, Eindhoven University of Technology, Eindhoven, The Netherlands
Email: l.pel@tue.nl

Abstract

Sodium sulfate is one of the most damaging and complex salts typically involved in the deterioration of our architectural heritage. One of the main difficulties is to determine which of its crystalline phases, i.e., thenardite, mirabilite or the metastable heptahydrate, will precipitate under certain conditions. Indeed, there is a significant range of temperature and relative humidity in which these phases can crystallize. Furthermore, one precipitated crystalline phase may under certain conditions transform to another one. Here, we show that NMR can be successfully used to non-destructively define the phase being precipitated. We investigate delamination of Ançã limestone due to sodium sulfate crystallization, a type of decay which is representative of those occurring in real constructions. The decay was achieved during isothermal drying of stone specimens under different environmental conditions. The work allowed concluding that mirabilite and heptahydrate can both be responsible for this type of decay in different conditions. The heptahydrate tends to crystallize when there is not previous presence of mirabilite crystals in the porous material.

Keywords

salt decay – soluble salts - sodium sulfate – mirabilite – thenardite – heptahydrate - Ançã limestone – NMR

Introduction

Salt crystallization is a very harsh and frequent decay mechanism of the porous materials that constitute our architectural heritage. For salts whose solubility is temperature-dependent crystallization can take place by temperature changes but, typically, it takes place due to evaporative drying processes.

Among the salts found in situ, sodium sulfate is one of the most damaging (Schaffer 1932, Arnold 1976, Price and Brimblecombe 1994, Goudie and Viles 1997, Hamilton and Hall 2008). Its phase diagram is given in Figure 1. As seen, three (main) distinct crystalline phases can be identified: mirabilite ($Na_2SO_4.10H_2O$), thenardite (Na_2SO_4), and also the metastable heptahydrate ($Na_2SO_4.7H_2O$). The heptahydrate phase was largely "forgotten" and almost overlooked in studies related with salt damage mechanisms during the last century (Hamilton et al. 2008, Saidov 2012). However, in the last few years, research has shown that this metastable phase can also be formed within the pores of several porous building materials (Rijniers 2004, Saidov 2012). Hence, heptahydrate should also be incorporated in physical theories of salt crystallization damage due to sodium sulfate (Hamilton and Hall 2008).

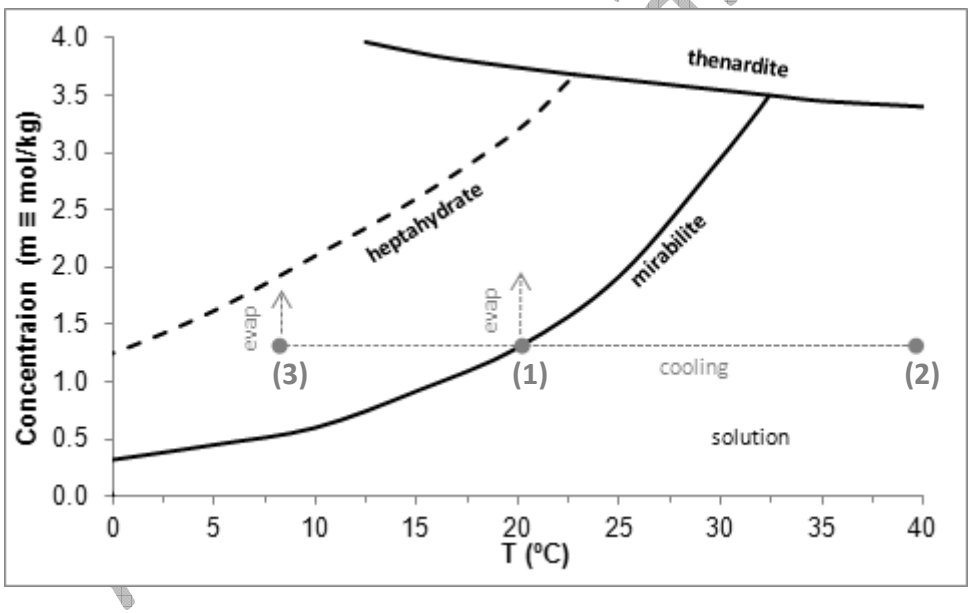

Figure 1. Phase diagram of sodium sulfate (Hartley et al. 1908): the bold solid lines are the solubility of mirabilite ($Na_2SO_4.10H_2O$) and thenardite (Na_2SO_4). The bold dashed line indicates the solubility of the metastable heptahydrate ($Na_2SO_4.7H_2O$). The grey lines indicate the experiments performed within this work

One of the main difficulties in the study of the damage caused by sodium sulfate is, therefore, to predict which of its three main phases will crystallize out. In particular, there are often doubts concerning which hydrated phase, mirabilite or heptahydrate is formed, as they can generally

crystallize under the same conditions of temperature and relative humidity (RH). At 20ºC, for instance, thenardite will only form below 77% RH. But both mirabilite and heptahydrate can form between 77% and 95.6% RH (Linnow et al. 2006).

An a posteriori identification of the chemical species, mirabilite or heptahydrate, is also not straightforward. The metastable heptahydrate may transform into mirabilite under certain conditions (Saidov 2012), and mirabilite easily converts into thenardite when exposed to a favorable atmosphere. The consequent difficulty in protecting and preserving the specimens poses, therefore, serious limits to chemical identification (Hamilton and Hall 2008). Powder X-ray diffraction is also unfeasible due to the time the samples need to be exposed to adverse conditions and the possibility of the phases change during the measurement. Recently Hamilton and Menzies (2010) reported the use of Raman spectra to identify mirabilite and heptahydrate. However, the authors had to resort to a laborious technique: the samples were stored and analyzed in sealed glass bottles to prevent dehydration, and the heptahydrate was stored and analyzed surrounded by some supernatant to avoid its conversion to mirabilite. In addition, this technique is still not able to identify the phases directly in a porous material. Using Nuclear Magnetic Resonance (NMR) one can study the transport of moisture and salt solutions in porous building materials (Kopinga and Pel 1994, Pel et al. 2002, Roels et al. 2004). NMR allows monitoring the moisture distribution in a drying specimen, giving direct indication on the salt decay mechanism. By also determining the salt concentration one can identify which sodium sulfate phase is formed in a porous material under certain environmental conditions (Rijniers 2004, Saidov 2012, Saidov et al. 2012). In relation to chemical techniques, NMR has the advantage that it can be used to monitor the alteration processes in real time and non-destructively. In addition, the measured concentration in a porous material can give a direct indication of the supersaturation being formed, giving information on the potential to damage due crystallization.

The resistance of porous building materials to salt crystallization is often evaluated by using crystallization tests such as the standardized ASTM test (ASTM 2013) which consist usually of wetting-drying cycles. In the case of sodium sulfate the damage is typically produced as the specimen is rewetted. Often it is found that this leads to massive disintegration of the material or other harsh decay patterns that do not reproduce the damages as found in situ. To overcome this situation Diaz Gonçalves and Brito (2014) introduced a new crystallization test which consists of a single isothermal drying event. It was performed on the Ançã limestone, a material which is widely used in monuments and is found to be very susceptible to salt decay (Costa and Delgado Rodrigues 2012). The specimen was filled with a saturated sodium sulfafe solution, 1.37 m [m ≡ mol/kg] at 20ºC, and afterwards dried at 50% RH and 20ºC. In this particular crystallization test, a delamination pattern was found which is similar to those observed in the field (Figure 2).

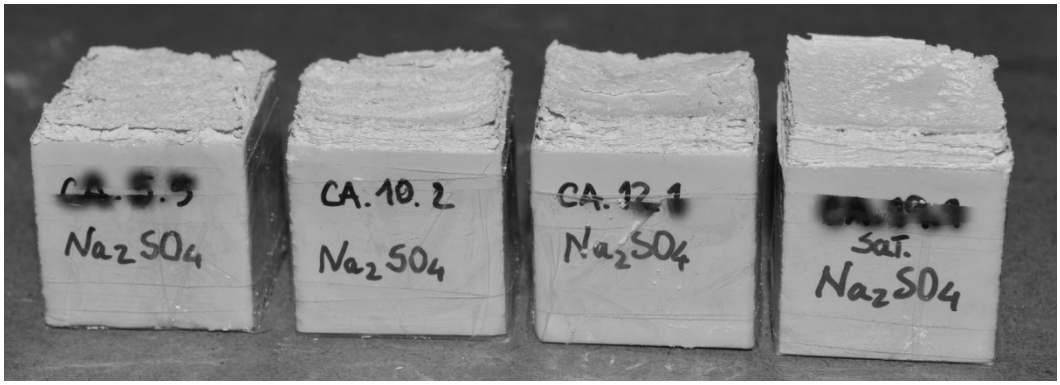

Figure 2. Delamination as seen after a single isothermal drying event of Ançã limestone at 20ºC and 50% RH with sodium sulfate solutions of different concentration: 0.37 m, 0.78 m, 0.96 m and 1.37 m, from left to right (image after dehydration)

In the present work we have used NMR to study the decay patterns of Ançã limestone due to sodium sulfate crystallization during isothermal drying under different environmental conditions. The main objectives were to investigate which is(are) the crystalline phase(s) associated to the delamination pattern, and whether distinct decay patterns arise when a different phase crystallizes.

The article is organized as follows. First, the materials and the methods used in the experiments are described. Then, the results of these experiments are presented and discussed and in the last section the main conclusions of the work are listed.

Materials and Methods

Materials

In this study we have used the Ançã limestone, which is a soft and fine-textured stone from Cantanhede region (Portugal) that can be found in many important buildings and monuments (Costa and Delgado Rodrigues 2012). The main hygric properties of this limestone are depicted in Table 1 and the pore size distribution, as measured by mercury intrusion porosimetry (MIP), is shown in Figure 3. As can be seen, it is a rather porous stone with a single modal pore size of 0.35 µm

Table 1. Capillary porosity (P), saturation coefficient (S), capillary water absorption coefficient (WAC) and vapour diffusion equivalent air layer thickness (Sd) of Ançã limestone, as measured by RILEM (1980) procedures

P (%)	S (%)	WAC ($kg\ m^{-2}\ s^{-1/2}$)	Sd (m)
22.90	86.70	0.15	0.40

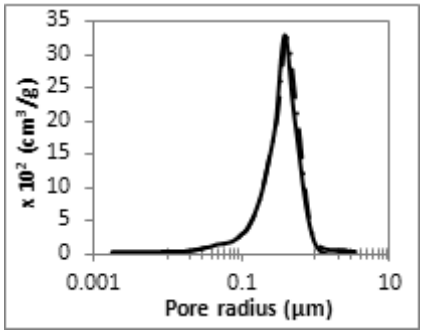

Figure 3. The measured pore size distribution of Ançã limestone by MIP (ASTM 2010): the modal pore radius is 0.35 μm

NMR fundamentals

NMR is a non-destructive imaging technique for quantitative mapping of certain chemical elements in materials. Its immense possibilities justified already the attribution of five Nobel Prizes in the last 50 years (Nobel Prize 2013). NMR has been used in medicine since the 1980s and, more recently, it has proven to be also suitable to study transport processes in porous building materials. In the last case, however, the measurement of the NMR signal is not straightforward because porous building materials contain magnetic impurities such as ferromagnetic ions. Specific experimental procedures are therefore needed, and specially adapted NMR machines have to be used (Kopinga and Pel 1994, Pel and Huinink 2012).

In NMR techniques, the specimen is placed in a strong magnetic field B_0, which causes the individual magnetic moments of the nuclei in the molecules to align. Radio frequency (RF) pulses at the resonance frequency of the nuclei are then used to apply a secondary oscillating magnetic field $B_1 << B_0$ perpendicular to B_0. B_1 will cause the magnetic moments to rotate away from their equilibrium position. At the termination of the RF pulse, the nuclei return to equilibrium, in a process called relaxation, by emitting electromagnetic radiation and by re-transferring the energy to the surrounding molecules. This emission of energy is what is observed as NMR signal.

To allow spatial discrimination, a magnetic gradient is applied. Hence the protons in the material will have a Larmor frequency that depends on their position. RF pulses at the appropriate frequency are then used to measure the density of the nuclei at a given position.

Experimental technique

The experimental setup is given in Figure 4. This NMR setup is based on an iron-cored electromagnet that produces a magnetic field of 0.78 T. Anderson gradient coils generate a

constant gradient of 0.3 T/m over this main field in the vertical direction. This allows a resolution of 1 mm in this direction.

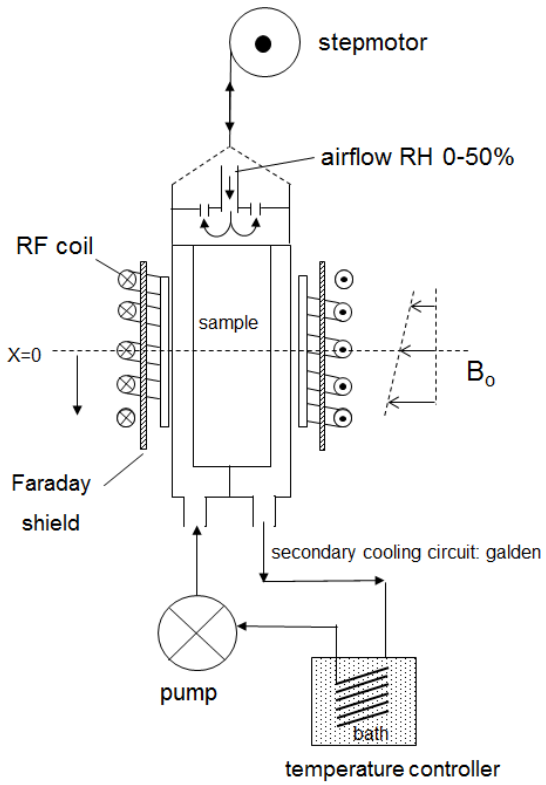

Figure 4. A schematic diagram of the NMR setup used for the drying experiments

The Ançã limestone specimens used in this study were cylinders with a diameter of 18 mm and a length of 25 mm. The specimens were all capillary saturated with a 1.37 m sodium sulfate solution by partial immersion during one day at 20ºC. Afterwards they were wrapped in Teflon tape except for the top surface which was left uncovered. The specimens were then placed in the NMR sample-holder, where their top surface was exposed to airflow of 1 l/min with controlled temperature and RH. In this way, a one-dimensional drying process (towards the open top of the specimens) was created. NMR scans were carried out along the length of the specimens with the help of a step motor which moved them vertically. It took about 83 seconds to determine the hydrogen and sodium contents at each position. Measuring an entire profile for the 25 mm length specimens took around 50 minutes. Since the duration of a typical drying experiment is several days, the variations occurring during a single scan could be neglected.

Because the measurement of each point was minimized in time to avoid influence on the profile, error of concentration measurement is in the order of ±0.25 m. However, for the interpretation of the data we need to observe differences in concentrations which are over 1.00 m to 2.00 m and, hence, beyond the resolution error.

The temperature was controlled by flowing a fluorinated heat transfer fluid (Galden©) through a heat exchanger in the wall of the sample-holder. The fluid contains no hydrogen or sodium, therefore no unwanted background signal in NMR measurements is acquired. The RH was controlled by using a special humidifying machine that can create an air flow at any given flow rate and HR ranging from 0 to 100%, with an error of HR +/-0.5%. In order to generate a certain HR two air flows of 0% and 100% HR are mixed at a desired proportion.

The experimental conditions used in this work are indicated in Table 2. Two of the experiments were performed at 20ºC with two different RH (Test A and Test B) whereas in the other tests the specimens were pre-heated at 40ºC (Test C and Test D).

Table 2. The testing conditions: the temperature used in the pre-heating phase and the drying phase are indicated, as well as the RH used in the experiment.

Test	Environmental conditions		
	Pre-heating (ºC)	During drying	
		Temperature (ºC)	RH (%)
A	-	20	50
B	-	20	0
C	40ºC	20	0
D	40ºC	7.5	0

Because drying with soluble salts could take a long time, a criterion was defined that the experiments should stop when the moisture content of the material was around 40%.

In the cases where delamination took place, the thickness of the laminae was estimated by optical profilometry using a Talysurf CLI 1000 instrument, by Taylor Hobson, equipped with a non-contact CLA gauge with vertical range of 3 mm, vertical resolution of 100 nm, a lateral resolution of 5 µm and a measuring slope of 13º. These thickness values should be considered as indicative; they represent typically the maximum thickness, as the thinner laminae are too fragile to be removed.

Results and Discussion

Test A: 20ºC and 50% RH

In the initial test the environmental conditions were kept identical to those where the Ançã delamination pattern (Figure 2) was originally observed in larger specimens (Diaz Gonçalves and Brito 2014), i.e. 20ºC and 50 % RH. This initial condition corresponds to point (1) in the phase diagram of Figure 1. The measured moisture, i.e., the moisture saturation, and ion concentration profiles are shown in Figure 5. The ion concentration profiles are obtained by

dividing the measured Na-ion content profiles by the corresponding moisture profiles. An image from the specimen at the end of the test showing the damage is also given in the figure.

From the moisture profiles (Figure 5a), it is seen that initially the specimen dried homogenously and no receding drying front was observed. This indicates the so-called stage I of drying, where drying front is always at the surface of the specimen. During this stage, ion will be transported to the surface by advection (Huinink et al. 2002, Pel et al. 2002) and will accumulate near the surface.

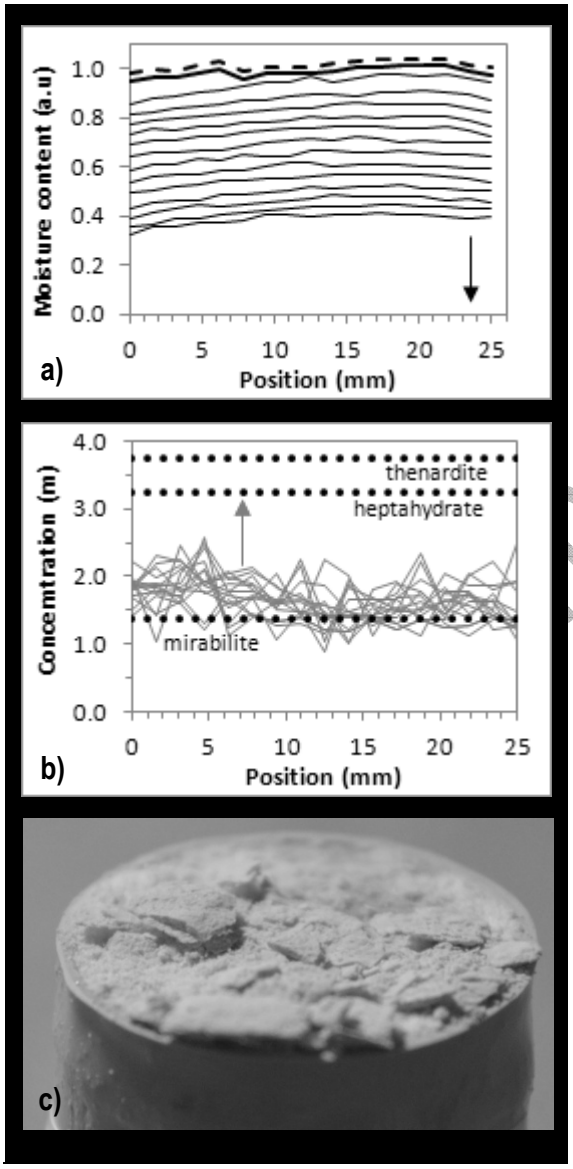

Figure 5. Test A: Results of drying at 20ºC and 50% RH after the specimen was initially saturated with 1.37 m Na_2SO_4 solution at 20ºC: a) moisture profiles, b) ion concentration profiles, c) image of the test specimen after the experiment. The profiles were measured every 12 h for a total time of 157 h and the arrows indicate the time evolution. The dotted lines corresponding to mirabilite, heptahydrate and thernardite concentration were drawn based on the phase diagram of Figure 1 for the given drying temperature

As can be seen from the concentration profiles (Figure 5b) these remained approximately constant throughout the specimen near the initial concentration. As the moisture profiles decrease at the same time, this means that in order to have a constant concentration the Na-content has to decrease. Since we have advection of ions to the surface during drying, this indicates that, in this particular case, the crystallization rate for mirabilite near the surface was high enough as no relevant increase in the concentration near the surface was verified. And, indeed, at the drying side of the specimen (position = 0 mm), sodium concentration is only slightly higher than in the rest of the specimen.

At the end of the experiment it was seen that crystallization gave rise to delamination of the stone, together with some efflorescence. The measured lamina thickness was of 0.5 to 0.8 mm. The subsequent dehydration of the crystals and transport of the specimen (after the end of the experiment) led to the breaking of the laminae and, so, the surface of the specimen was disintegrated (Figurer 5c).

Test B: 20ºC and 0% RH

In a second test we have kept the initial condition the same as in the previous Test A (point 1 in the phase diagram of Figure 1), but changed the boundary condition to 0% RH. The measured moisture and the ion concentration profiles are shown in Figure 6. As can be seen from the moisture profiles (Figure 6a) also in this case initially the specimen dried homogenously, indicating stage I drying. However, under these drying conditions after some time a receding drying front occurred, which corresponds to the starting of drying stage II. From the measured concentration profiles (Figure 6b), it is seen that concentration remained approximately constant during stage I, near mirabilite solubility line indicating that also in this case mirabilite was being formed near the surface. With the beginning of stage II, when a receding drying front was observed, a strong increase in concentration near the surface was observed. These high concentrations could be associated to:

i. Dehydration of mirabilite to thenardite, when the feed of solution is interrupted due to the receding of the drying front. If the salt were dissolved in the excess water, the observed high supersaturations could perhaps occur. This kind of dehydration was already observed in direct measurements during drying of sodium sulfate solutions in Derluyn et al. (2011) research. The same was also observed in porous materials (Saidov 2012).
ii. Occurrence of disconnected clusters of solution, which are left behind as the drying front recedes (Yiotis et al. 2001). Evaporation proceeds locally from these clusters, in which the supersaturation rises so much that it reaches the solubility of thenardite. Therefore, thenardite could eventually crystallize directly from solution at these positions. Directed precipitation of thenardite at high supersaturation in building stones was previously reported, for example, by Doehne et al. (2002). The occurrence of disconnected clusters was already studied in other research works (Gupta 2013, Saidov 2012, Kopinga and Pel 1994, Huinink et al. 2002)

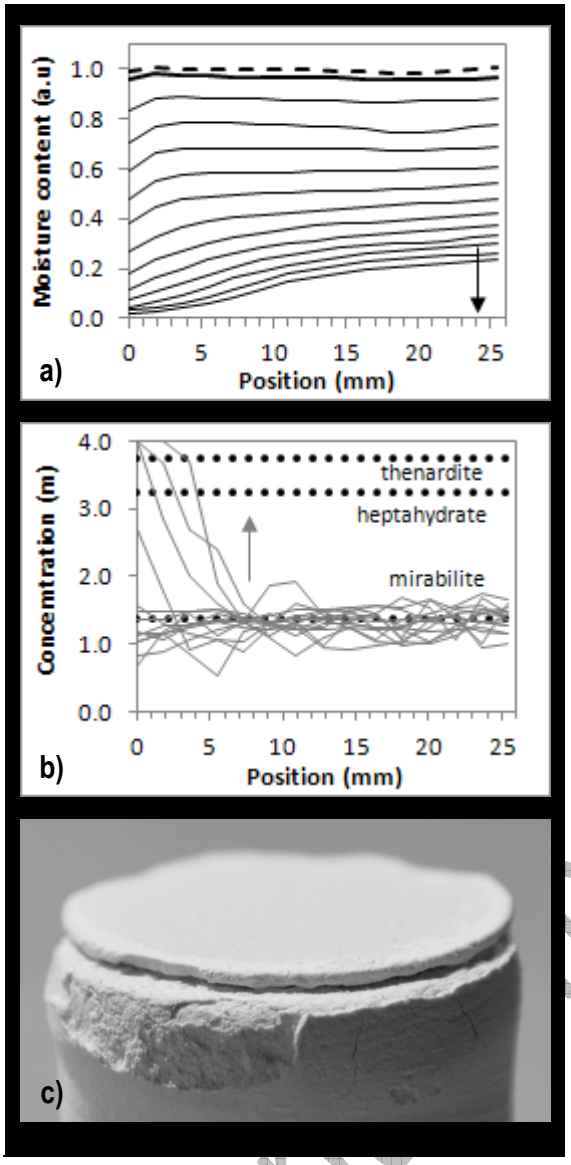

Figure 6. Test B: Results of drying at 20ºC and 0% RH after the specimen was initially saturated with 1.37 m Na_2SO_4 solution at 20ºC: a) moisture profiles, b) ion concentration profiles, c) image of the test specimen after the experiment. The profiles were measured every 3 h for a total time of 41 h and the arrows indicate the time evolution. The dotted lines corresponding to mirabilite, heptahydrate and thernardite concentration were drawn based on the phase diagram of Figure 1 for the given drying temperature

The question of why liquid clusters are not detected in the moisture profiles, in association with the high supersaturations depicted in the concentration profiles, arises in relation to both hypotheses. The explanation may be that these are very low moisture contents, which is in agreement with the fact that it is precisely because of a reduction in moisture content that the evaporation front eventually recedes during drying.

A delamination pattern arose in this test, as seen in Figure 6c. Here, a thicker layer detached first, followed by other thinner layers. Delamination seems to be related to mirabilite crystallization because the solubility of thenardite was only reached, during the subsequent stage II. The thickness of the first detached lamina is of 0.6 to 0.7 mm.

Test C: 20ºC and 0% RH, with pre-heating at 40ºC

As to exclude the possibility that in the previous Tests A and B there were already nucleation sites available, we have conducted additional tests in which the specimen was pre-heated. In the first experiment we repeated the previous experiment (Test B). However after the specimen was saturated at 20ºC, the specimen was heated up to 40ºC for some time (segment $\overline{12}$ in Figure 1) and cooled down again to 20ºC (segment $\overline{21}$ in Figure 1). During preheating, all nucleation sites (microcrystals of mirabilite) that could still be present in the system would dissolve. Hence, assuming no influence of the porous medium on crystallization, we would have a pure solution in the material. According the Ostwald's rule of stages (Bohm 1985) which states that least stable polymorph crystallises first, no formation of mirabilite was expected to occur in this case.

The measured moisture saturation and salt concentration profiles are shown in Figure 7. As can be seen, the moisture profiles (Figure 7a) show that during drying the water content decreased homogeneously throughout the specimen and no drying front was observed until the end of the experiment. This corresponds to stage I conditions, as discussed previously. The concentration initially increased slowly and a broad peak was build up near the top (Figure 7b), indicating that advection was only slightly dominant over diffusion. During this experiment the concentration near the surface increased to the heptahydrate solubility, indicating that heptahydrate crystals could be formed.

There are several reasons that can invoke formation of mirabilite from a solution, i.e., presence of initial nucleation site as micro crystals of mirabilite, interaction of the solution with a pore matrix or an influence of chemical contaminants present in the pores. However, it is obvious that pre-heating eliminates the reasons provoking formation of mirabilite directly from the solution. This knowledge is important in further understanding on the decay patterns of Ançã limestone stone by sodium sulfate.

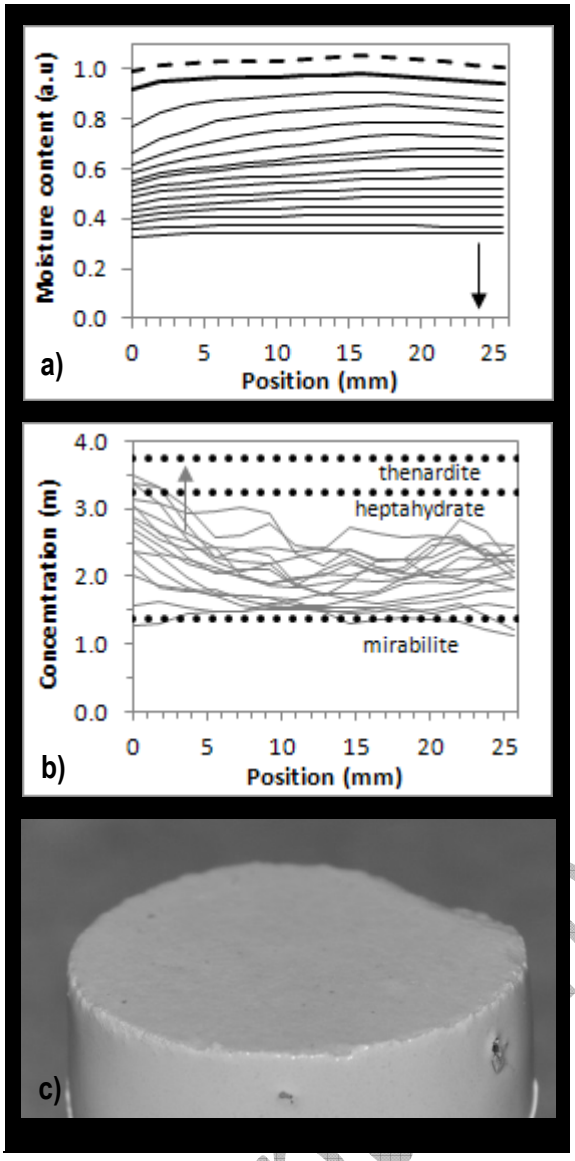

Figure 7. Test C: Results of drying at 20ºC and 0% RH after the specimen was initially saturated with 1.37 m Na_2SO_4 solution at 20ºC, heated up to 40ºC and cooled down again to 20ºC: a) moisture profiles, b) ion concentration profiles, c) image of the test specimen that shown no damage. The profiles were measured every 12 h for a total time of 170 h and the arrows indicate the time evolution. The dotted lines corresponding to mirabilite, heptahydrate and thernardite concentration were drawn based on the phase diagram of Figure 1 for the given drying temperature

Test D: 7.5ºC and 0% RH, with pre-heating at 40ºC

In order to investigate the possible damage due to heptahydrate, we have repeated the experiment with pre-heating (Test C). However the specimen was in this case cooled down to 7.5ºC (segment $\overline{23}$ in Figure 1) and subsequently dried. The measured moisture content and salt concentration profiles are shown in Figure 8.

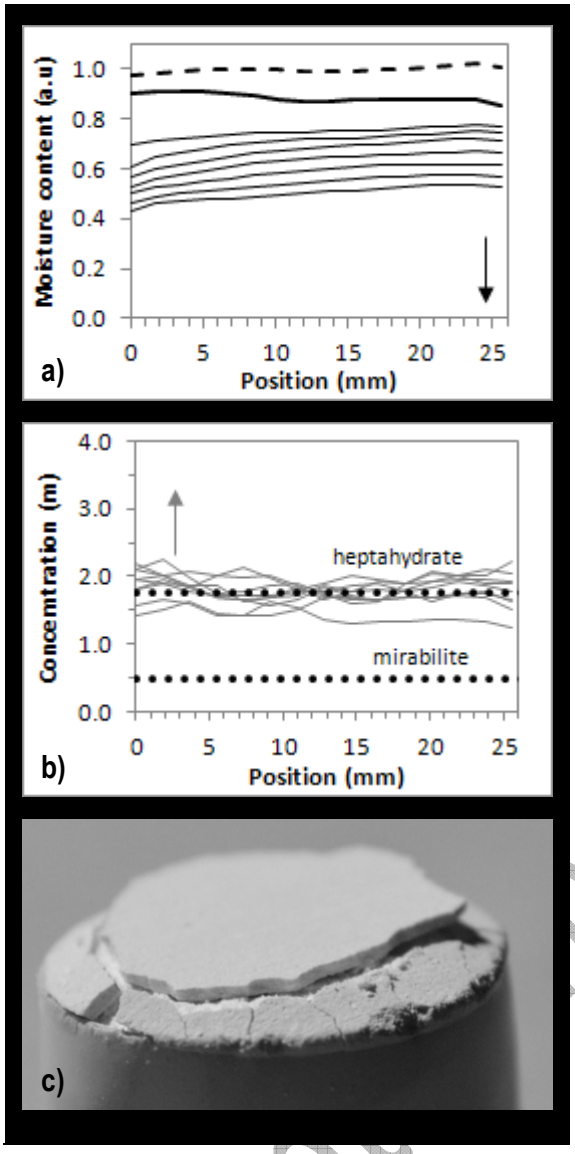

Figure 8. Test D: Results of drying at 7.5ºC and 0% RH after the specimen was initially saturated with 1.37 m Na_2SO_4 solution at 20ºC, heated up to 40ºC and cooled down to 7.5ºC: a) moisture profiles, b) ion concentration profiles, c) image of the test specimen after the experiment. The profiles were measured every 12 h for a total time of 92 h and the arrows indicate the time evolution. The dotted lines corresponding to mirabilite and heptahydrate concentration were drawn based on the phase diagram of Figure 1 for the given drying temperature

As seen, the specimen dried homogeneously under stage I conditions (Figure 8a), as discussed previously. Concentration profiles shows that almost immediately after the drying has started the concentration in the specimen has reached the heptahydrate solubility throughout the specimen (Figure 8b). As the concentration profiles remained approximately constant, this indicates that also in this particular case the crystallization rate for heptahydrate near the surface was high enough as no increase in the concentration near the surface was observed. At the end of the experiment a peripheral fissure had developed on the surface of the specimen (Figure 8c), corresponding to the detachment of a stone layer with thickness of around 0.6-0.7 mm. In this case, the damage was pure due to the initial formation of heptahydrate.

Discussion of crystallizing phases and decay patterns

In Table 3, a summary of the decay patterns and crystal phases present in the material at the end of each experiment are shown. The drying stage (I or II) during which those crystal phases precipitated is indicated.

Table 3. Summary of the decay patterns and corresponding crystallizing phases

Test	Environmental conditions	Drying stage [(1)]	Decay patterns		Crystal phases
			Type	Description	
A	20ºC 50% RH	Stage I	Efflorescence and delamination	Efflorescence deposition followed by delamination of the stone.	Mirabilite
B	20ºC ≈ 0% RH	Stage I + Stage II	Delamination	Delamination of a thicker first layer followed by other thinner layers.	Mirabilite + Thenardite
C	20ºC* ≈ 0% RH	Stage I	No decay was observed		Heptahydrate
D	7.5ºC* ≈ 0% RH	Stage I	Delamination	Peripheral fissure corresponding to delamination of a surface layer.	Heptahydrate

(*) Pre-heating at 40ºC

[(1)] Stage I – surface evaporation; Stage II – the drying front is inside the material

The results in Table 3 show that the main decay pattern of the Ançã limestone was delamination. This consists in the detachment of stone layer(s) pushed by subflorescence. Delamination was due to mirabilite crystallization in two cases (Tests A and B) and to heptahydrate crystallization in the other (Test D). This means that both phases are able to generate such a crystallization pressure as to be able to cause a similar type of damage to this limestone.

In salt decay literature, damage to porous building materials in this range of temperatures is usually attributed to mirabilite crystallization, because mirabilite is the equilibrium phase in contact with a saturated sodium sulfate solution below 32.4ºC. However, in the last few years, some authors have suggested that the metastable heptahydrate, which may also crystallize from solution below 32.4ºC, could also be relevant in this context. Rijniers (2004) observed heptahydrate crystallization inside the pores of Savonière stone, fired-clay brick and calcium silicate brick during temperature-induced crystallization experiments. Latter, Saidov (2012) also observed heptahydrate crystallization within evaporation-induced crystallization experiments at

7.5ºC and 5% RH (with pre-heating at 40ºC) on fired-clay brick, Indiana limestone and Cordova Cream limestone. NMR allowed these observations, which were based on the analysis of moisture and sodium distribution profiles, as we did in the present work.

Here, we show that the crystallization of heptahydrate can be associated with the most harmful feature of salt decay, i.e., the occurrence of physical damage in the porous material. But perhaps the most interesting observation of this work is that the same degradation pattern (delamination) can result both from the crystallization of mirabilite (Tests A and B) and of heptahydrate (Test D).

The occurrence of one phase or another is also not associated to any variation in drying kinetics (Figure 9) that could justify the differences in supersaturation observed in Figures 5b, 6b and 8b. As seen in Figure 9, the drying kinetics does not define the crystallization pathway. Both heptahydrate and mirabilite formation were observed for similar drying kinetics, but two different drying kinetics were also observed for the same crystallizing phase (mirabilite). A similar phenomenon, i.e., independence of crystallization kinetics in relation to the phase of sodium sulfate being formed was also observed by Saidov (2012) during drying and cooling (Saidov et al. 2012). The high supersaturations, i.e., above the solubility of mirabilite, are always associated to the existence of a pre-heating period (Tests C and D, in the present case). This pre-heating period was used to ensure that no crystallization would take place before the actual drying started. That could lead to the formation of mirabilite crystals and, thus, prevent further precipitation of the heptahydrate (because the two phases cannot coexist). Therefore, the fact that a high supersaturation has never been achieved without pre-heating (Tests A and B) suggests that heptahydrate tends to crystallize first when there is not previous presence of mirabilite. This is in accordance with Ostwald's rule of stages (Bohm 1985), which states that the preferred crystalline phase is the one with highest solubility.

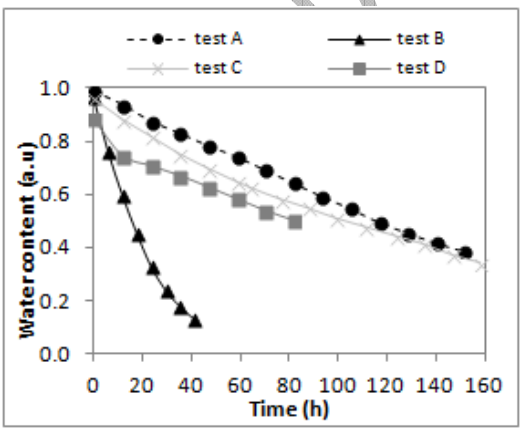

Figure 9. Drying kinetics and crystal phase present in the material at the end of each experiment: mirabilite (black triangles and circles); heptahydrate (light grey xx); heptahydrate or thenardite could crystallize at a later stage (dark grey squares)

The presence of crystals in the porous material and their nature determine, thus, whether it is mirabilite or the heptahydrate that will crystallize from solution. The two phases did not result in different type of damage for the Ançã limestone. In the future, it will be interesting to verify if the same happens with other materials. Therefore, in forthcoming salt decay research, the pre-existence of crystals in the porous material should be taken into account. It seems appropriate to consider both the presence of thenardite and of mirabilite. Indeed, the pre-existence of crystals of an equilibrium form is likely in the porous materials of the architectural heritage, given the large periods of time involved. Which of the two, thenardite or mirabilite, depends at least on the environmental conditions, which will vary with the geographic location and season.

Conclusions

Sodium sulfate crystallization in Ançã limestone was investigated under four environmental conditions. The main decay pattern was delamination, i.e., the detachment of thin stone layers pushed by subflorescence. Both mirabilite and heptahydrate were responsible for this type of decay in different conditions, respectively. The heptahydrate tended to crystallize first when there was not previous presence of mirabilite crystals.

NMR proved to be a valuable tool for the identification of the crystalline phases that precipitate at each depth and moment. This identification is based on the analysis of moisture content profiles and sodium concentration profiles obtained by NMR measurement of the hydrogen and sodium contents in different points of the specimens and different moments of the drying.

Acknowledgements

This work was supported by national funds, under the research project DRYMASS [ref. PTDC/ECM/100553/2008], through the Portuguese Fundação para a Ciência e a Tecnologia (FCT) and the Laboratório Nacional de Engenharia Civil (LNEC). It was performed at the Department of Applied Physics of Eindhoven University of Technology (the Netherlands). The authors thank the help of Jinping Han, Sonia Gupta and Pim Donkers for their assistance with NMR setup. The authors would like to acknowledge also the contributions of José Costa and José Delgado Rodrigues.

References

Arnold A (1976) Behaviour of some soluble salts in stone deterioration. In: *2nd international symposium on the deterioration of building stone*, Athens (Greece), pp. 27-36.

ASTM D4404-10 (2010) Standard test method for determination of pore volume and pore volume distribution of soil and rock by mercury intrusion porosimetry.

ASTM C88-13 (2013) Standard test method for soundness of aggregates by use of sodium sulfate or magnesium sulphate.

Bohm J (1985) The history of crystal growth. *Acta Physica Hungarica* 57(3–4): 161 – 178.

Costa D and Delgado Rodrigues J (2012) Consolidation of a porous limestone with nanolim. In *12th international congress on the deterioration and conservation of stone*, Oral Presentations – Methods and Materials of Cleaning, Conservation, Repair, Maintenance; Logistics and Planning, session X, New York, USA, 22-26 October.

Derluyn H, Saidov TA, Espinosa-Marzal RM, Pel L, Scherer GW (2011) Sodium sulfate heptahydrate I: The growth of single crystals. *Journal of Crystal Growth* 329(1): 44-51.

Diaz Gonçalves T, Pel L, Delgado Rodrigues J (2007) Drying of salt-contaminated masonry: MRI laboratory monitoring. *Environmental Geology* 52(2): 293–302.

Diaz Gonçalves T and Brito V (2014) Alteration kinetics of natural stones due to sodium sulphate crystallization: can reality match experimental simulations? *Environmental Earth Sciences*. DOI 10.1007/s12665-014-3085-0.

Doehne E, Selwitz C, Carson DM (2002) The damage mechanism of sodium sulfate in porous stone. In: *SALTeXPERT Meeting* (ed Stefan Simon and Miloš Drdácký), Prague.

Goudie A and Viles H (1997) *Salt Weathering Hazard*. John Wiley & sons, Chichester, UK. ISBN 0-471-95842-5.

Gupta S (2013) *Sodium chloride crystallization in drying porous media: influence of inhibitor.* PhD Thesis, Eindhoven University of Technology, The Netherlands.

Hamilton A and Hall C (2008) Sodium sulphate heptahydrate: a synchrotron energy-dispersive diffraction study of an elusive metastable hydrated salt. *Journal of Analytical Atomic Spectrometry* 23: 840–844.

Hamilton A, Hall C, Pel L (2008) Sodium sulphate heptahydrate: direct observation of crystallization in a porous material. *Journal of Physics D: Applied Physics* 41.

Hamilton A and Menzies RI (2010) Raman spectra of mirabilite, $Na_2SO_4.10H_2O$ and the rediscovered metastable heptahydrate, $Na_2SO_4.7H_2O$. *Journal of Raman Spectroscopy* 41(9): 1014–1020.

Harley H, Jones BM, Hutchison GA (1908) The spontaneous crystallization of sodium sulphate solutions. *Journal of the Chemical Society* 93: 825-833.

Huinink HP, Pel L, Michels MAJ (2002) How ions distribute in a drying porous medium: a simple model, *Physics of Fluids* 14: 1389-1395.

Kopinga K and Pel L (1994) One dimensional scanning of moisture in porous materials with NMR. *Review of Scientific Instruments* 65(12): 3673-3681.

Linnow K, Zeunert A, Steiger M (2006) Investigation of sodium sulphate phase transitions in a porous material using humidity-and-temperature-controlled X-ray diffraction, *Analytical Chemistry* 78: 4683-4689.

Nobel Prize (2013) Isidor Isaac Rabi – Facts. Felix Bloch – Facts. E. M. Purcell – Facts. Richard R. Ernst – Facts. Kurt Wüthrich – Facts. Paul C. Lauterbur – Facts. Sir Peter Mansfield – Facts. Nobel Media AB (accessed 18 November 2013). Available at: http://www.nobelprize.org/nobel_prizes/physics/laureates/1944/rabi-facts.html

http://www.nobelprize.org/nobel_prizes/physics/laureates/1952/bloch-facts.html,
http://www.nobelprize.org/nobel_prizes/physics/laureates/1952/purcell-facts.html,
http://www.nobelprize.org/nobel_prizes/chemistry/laureates/1991/ernst-facts.html,
http://www.nobelprize.org/nobel_prizes/chemistry/laureates/2002/wuthrich-facts.html,
http://www.nobelprize.org/nobel_prizes/medicine/laureates/2003/lauterbur-facts.html,
http://www.nobelprize.org/nobel_prizes/medicine/laureates/2003/mansfield-facts.html

Pel L, Huinink H, Kopinga K (2002) Ion transport and crystallization in inorganic building materials as studied by nuclear magnetic resonance. *Applied Physics Letters* 81(15): 2893-2895.

Pel L and Huinink HP (2012) *Building Materials Studied by MRI*, *Encyclopedia of Magnetic Resonance*. John Wiley & Sons, Ltd (DOI: 10.1002/9780470034590.emrstm1294)

Price C and Brimblecombe P (1994) Preventing salt damage in porous materials. *Preprints of the Contributions to the Ottawa Congress Preventive Conservation: Practice, Theory and Research* (ed Roy A and Smith P). International Institute for Conservation of Historic and Artistic Works, London, UK, 90-93.

Rijniers LA (2004) *Salt crystallization in porous materials: an NMR study*. PhD Thesis, Eindhoven University of Technology, The Netherlands.

RILEM TC 25-PEM (1980) Recommended tests to measure the deterioration of stone and to assess the effectiveness of treatment methods, *Materials and Structures* 13: 176-179 (test No. I.1 “Porosity accessible to water”), 194-197 (test No. II.1 “Saturation coefficient”, 197-199 (test No. II.2 “Coefficient of water vapour conductivity”), 208-209 (test No. II.6 “Water absorption coefficient (capillarity)”, Paris.

Roels S, Carmeliet J, Hens H et al. (2004) A comparison of different techniques to quantify moisture content profiles in porous building materials. *Journal of Thermal Envelope and Building Science* 27(4): 261–276.

Saidov T (2012) *Sodium sulfate heptahydrate in weathering phenomena of porous materials*. PhD Thesis, Eindhoven University of Technology, The Netherlands.

Saidov T, Espinosa-Marzal R, Pel L, Scherer GW (2012) Nucleation of sodium sulfate heptahydrate on mineral substrates studied by nuclear magnetic resonance, *Journal of Crystal Growth* 338(1): 166–169.

Schaffer RJ (1932) The weathering of natural building stones. Building Research Special Report 18, reprinted with slight amendments 1933. His Majesty's Stationery Office, London.

Yiotis AG, Stubos AK, Boudouvis AG et al. (2001) A 2-D pore-network model of the drying of single-component liquids in porous media. *Advances in Water Resources* 24: 439-460.